Structure, Vol. 13, 1365–1373, September, 2005, ©2005 Elsevier Ltd All rights reserved. DOI 10.1016/j.str.2005.06.018

NF-κB RelB Forms an Intertwined Homodimer

De-Bin Huang, Don Vu, and Gourisankar Ghosh*
Department of Chemistry and Biochemistry
University of California, San Diego
9500 Gilman Drive
La Jolla, California 92093

Summary

The X-ray structure of the RelB dimerization domain (DD) reveals that the RelBDD assumes an unexpected intertwined fold topology atypical of other NF-κB dimers. All typical NF-κB dimers are formed by the association of two independently folded immunoglobulin (Ig) domains. In RelBDD, two polypeptides reconstruct both Ig domains in the dimer with an extra β sheet connecting the two domains. Residues most critical to NF-κB dimer formation are invariant in RelB, and Y300 plays a positive role in RelBDD dimer formation. The presence of RelB-specific nonpolar residues at the surface removes several intradomain surface hydrogen bonds that may render the domain fold unstable. Intertwining may stabilize the RelBDD homodimer by forming the extra β sheet. We show that, as in the crystal, RelB forms an intertwined homodimer in solution. We suggest that the transiently stable RelB homodimer might prevent its rapid degradation, allowing for heterodimer formation with p50 and p52.

Introduction

The dimeric NF-κB transcription factors play critical roles in diverse cellular processes, including adaptive and innate immunity, cell differentiation, proliferation, and apoptosis (Ghosh et al., 1998). Transcriptionally active NF-κB dimers are formed by combinatorial association of five subunits, p50 (NF-κB1), RelA (p65), p52 (NF-κB2), c-Rel, and RelB, which share an approximately 300 residues long homologous element close to their N termini. This element, referred to as the Rel Homology Region (RHR), is responsible for DNA binding, dimerization, inhibitor binding, and nuclear localization. p50 and p52 are the processed products of precursor proteins p105 and p100, respectively (Baldwin, 1996; Ghosh et al., 1998). Although processing of both p105 and p100 is carried out by the proteasome, p105 processing is primarily constitutive, and p100 processing is primarily inducible (Ghosh and Karin, 2002). The mature NF-κB p50 and p52 subunits lack inherent transcriptional activation domains and function in vitro as repressors of transcription (Baldwin, 1996).

In most unstimulated cells, NF-κB dimers with transcriptional activation potential are inhibited by a class of inhibitor proteins known as IκB through the formation of stable IκB/NF-κB complexes that are unable to bind DNA. In response to NF-κB-inducing stimuli, such as the cytokines TNF-α and IL-1, IκB is phosphorylated by active IκB kinase (IKK), leading to subsequent ubiquitination and 26S proteasome-dependent degradation. IκB degradation releases free NF-κB, which then enters the nucleus, binds cognate DNA sequences within gene enhancer elements, and activates transcription (Ghosh and Karin, 2002; Karin and Ben-Neriah, 2000). This process is now referred to as the canonical NF-κB activation pathway. The primary NF-κB effectors of this canonical pathway are the RelA/p50 and c-Rel/p50 heterodimers.

The X-ray structures of several NF-κB dimers involved in the canonical pathway are known. These include the p50, p52, p65, and c-Rel homodimers and the p50/p65 heterodimer (Chen et al., 1998a, 1998b; Cramer et al., 1997; Ghosh et al., 1995; Huang et al., 2001; Muller et al., 1995). These structures have shown that the RHR forms two-folded domains connected by a flexible linker with a small, unstructured segment containing the basic type I nuclear localization signal (NLS) at its C terminus. The C-terminal Ig-like domain of approximately 100 amino acids is wholly responsible for dimer formation. As a consequence, this domain is commonly referred to as the DD.

All of the NF-κB structures exhibit a common mechanism of dimer formation in which each monomer contributes symmetrical β strand elements that pack against each other to form a β sheet dimer interface. Roughly 12 side chains from each subunit mediate symmetrical (or pseudosymmetrical) intersubunit contacts (Figure 1A). These residues are highly homologous across the NF-κB family (Huang et al., 1997). The contribution of each of these residues in dimer formation has been studied by alanine scanning mutagenesis and by in vivo selection with p50 as a model system (de Lumley et al., 2004; Hart et al., 2001; Sengchanthalangsy et al., 1999). Results from these experiments reveal that only four of these interfacial residues, Y267, L269, D302, and V310, are critical for p50 homodimer formation. Except for Y267, these residues are identical in all NF-κB subunits. Tyrosine is substituted with a phenylalanine at the corresponding positions in p65 and c-Rel. Involvement of the hydroxyl groups of tyrosine in the cross subunit hydrogen bonding may explain why the p65 and c-Rel homodimers are weaker compared to the p50 homodimer. The identity of residues at the position corresponding to 254 of p50 may contribute additional regulation to the stability of NF-κB dimers (Huang et al., 1997).

Gene knockout experiments in mice showed that although each of these NF-κB family members carries out distinct functions (Gerondakis et al., 1999; Hoffmann et al., 2003; Sanjabi et al., 2000), knockout of the RelA subunit has the strongest phenotype. This subunit, the most important target for the canonical pathway, displays the most widespread biological function and is involved in activating expression of most genes that are involved in immune and inflammatory responses as well as rescue from apoptosis. In recent years, a new NF-κB activation pathway has been eluci-

*Correspondence: gghosh@ucsd.edu

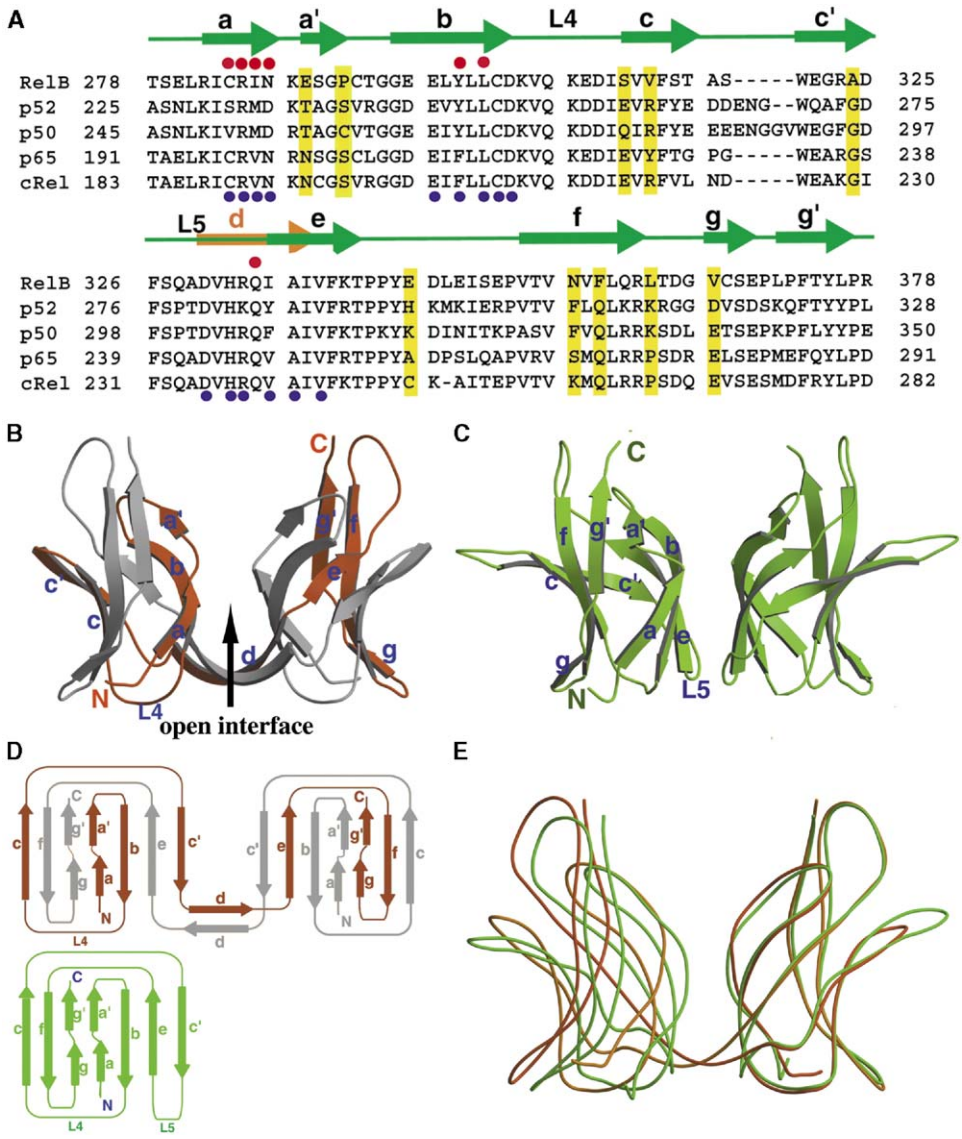

Figure 1. Primary Sequences and Secondary and Tertiary Structures of the Dimerization Domains of Murine NF-κB Family Members

(A) Sequence of dimerization domains of Rel/NF-κB family members. Secondary structural elements are indicated above the aligned sequences. Green arrows denote residues in β strands, and the orange arrows denote residues in the β strand only seen in RelBDD. Residues at the RelBDD homodimer open interface that contact the two Ig-like folds are marked by red circles. Residues that make subunit contacts at the dimer interfaces of all NF-κB dimmers, except the RelBDD homodimer, are shown below the aligned sequences by blue circles. Unique residues in RelBDD (yellow shade) are denoted. L4 and L5 are the loops that contact DNA.

(B) Ribbon presentation of the intertwined dimer of RelB.

(C) Ribbon presentation of the structure of the p50 homodimer.

(D) Folding pattern of the RelBDD/RelBDD dimer (top) and the canonical p50 DD (bottom).

(E) Backbone overlay of RelBDD (orange) and p50DD (green) by superposing one domain from each dimer.

dated which requires a distinct class of inducers such as LTβ, BAFF, and CD40. These inducers activate the noncanonical pathway and generate the RelB/p52 heterodimer (Claudio et al., 2002; Coope et al., 2002; Dejardin et al., 2002; Senftleben et al., 2001; Xiao et al., 2001).

Although the *relb* gene was identified around the same time as other NF-κB family members, the mechanism of its biological mode of action has remained elusive compared to that of the other members. This is in part due to the fact that RelB does not share the common "Rel family" functional properties. No exclusive DNA binding activity has been found to date, suggesting that RelB may not form a stable, detectable homodimer in vivo (Ruben et al., 1992). RelB is also unable to form stable heterodimers with c-Rel and p65. To understand the preferential heterodimerization of p50 and RelB, the DD of RelB was extensively mutagenized (Ryseck et al., 1995). However, this study could not provide a clear conclusion. To our knowledge, the RelB subunit is unique to the noncanonical NF-κB activation pathways.

Remarkably, the residues at the RelB dimer interface are nearly identical to p50 and p52, enabling it to form heterodimers with these two family members, but not with itself or with the other members. Therefore, the regulation of combinatorial dimer formation seems to be controlled by residues at the interface as well as residues outside of the interface. In order to gain insight into the molecular basis for biological activity of RelB, we have determined the X-ray structures of both wild-type RelBDD and the RelBDD Y300S mutant.

Results and Discussion

Overall Structure of the RelB Dimerization Domain

The DDs of RelB, p50, and p52 are highly similar, sharing 52% sequence identity and 70% homology (Figure 1A). We observe that RelBDD crystallizes as a dimer. However, the architecture of the dimer interface is strikingly different compared to other NF-κB homo- and heterodimers (Figures 1B–1E). Structures of all other combinatorial NF-κB dimers known to date revealed that the association of two monomers involves independent Ig-like folds that contact one another symmetrically to form the dimer (Chen and Ghosh, 1999; Chen et al., 1998a, 1998b) (Figure 1C). The RelB homodimer, however, is an intertwined dimer that is composed of two RelBDD polypeptides that participate in the reconstruction of both Ig domains in the dimer and an extra β sheet consisting of two symmetrical β strands connecting the two domains (Figures 1B and 1D). The individual RelBDD Ig-folds are, however, identical to those of the other NF-κBDD structures. Intertwined dimers constitute a subclass of three-dimensional domain-swapped dimers. Eisenberg and coworkers first introduced the term three-dimensional domain swapping to describe the structure of diphtheria toxin; subsequently, this type of domain swapping has been found to be involved in several other cases (Bennett and Eisenberg, 1994; Liu and Eisenberg, 2002). It has been shown in many cases that the exchange of domains or subdomains requires a relatively unstable fold of the protein.

The RelB dimer is formed through the exchange of identical structural motifs composed of four β strands (aa′-b-c-c′) of one molecule and three strands (e-f-gg′) from the other. Two different interfaces result because of this domain swapping. The true subunit interface is essentially the Ig domain cores formed by the interactions of two β sheets. A second interface, referred to as the open interface, is formed by the interactions of the two folded domains (Figure 1B). This open interface is equivalent to the regular side-by-side NF-κB dimer interface, but it is significantly different due to the presence of the extra β sheet formed by the two new symmetrical "d" strands (Figures 1A, 1B, and 1D). These β strands form relatively tight turns in other NF-κB proteins, allowing each peptide chain to complete the single polypeptide Ig-like fold.

Comparison between RelB and p50 Dimer Interfaces

Overlaying the p50DD homodimer on the RelBDD homodimer requires more than 17° rotation and 5 Å translation to bring a second RelBDD over the homologous p50DD (Figure 1E). The overlay also reveals that the backbone and side chains of the secondary structural elements involved in the formation of the regular interface align nicely between p50DD and RelBDD, with the exception of only three side chains (Figure 2A). Y300 (corresponds to Y267 of p50), H332, and Q334 are the only side chains in RelB showing significantly different conformations compared to the corresponding side chains in p50 (Figure 2). Overall structural comparison reveals that the open dimer interface of the RelBDD homodimer is significantly open and that several water molecules occupy the interdomain space. Some of these water molecules are involved in bridging the two RelB domains. In regular NF-κB dimers, strands "a," "b," and "e" and loop 5 are involved in dimerization (Figure 1C). In RelBDD, loop 5 changed its conformation to a new β strand ("d") (compare Figures 2D and 2F). Only strand "a" and part of strand "b" participate in the interactions between the two Ig-like folds through the open interface. Consequently, in RelBDD, the total number of interdomain van der Waals contacts are few compared to other NF-κB dimers. As a further illustration of this point, the solvent-excluded surface area of the open interface in the RelBDD dimer is only about 900 Å^2. In comparison, the p50DD homodimer and the p50/p65 heterodimer bury approximately 1400 and 1500 Å^2 exposed surface area, respectively, upon subunit association. This marked reduction in the solvent-excluded surface area of the open interface in RelB is due to the fact that the new crossdomain "dd" antiparallel β sheet at the bottom of the molecule restricts the proper movement of the rest of the domain that is needed to form a compact subunit interface (Figures 2D, 2E, and 2F).

The RelBDD dimer has identical topology to that of a domain-swapped, intertwined mutant p50DD dimer. The domain swapping in this p50DD mutant is caused by only two amino acids changes, Y267M and V310M. The same β stands are exchanged to form the Ig domain, and the exchange occurs at identical positions in both cases. The hydrogen bonding pattern in the newly formed "dd′" β sheet is identical in both structures (Figures 2E and 2F). Domain swapping might be a conserved mechanism within the Rel family that compensates for the inability to form a normal side-by-side dimer.

In the RelBDD dimer, seven amino acids of each monomer are within 4 Å of the closest atoms of the opposing domain (Figure 1A), and there are only about ten van der Waals contacts and four hydrogen bonds directly involved in bridging the two domains. Most of these hydrogen bonds, however, appear to be quite weak, as evidenced by their large separations, poor geometry, and high temperature factors between the hydrogen bonded side chains (compare Figures 3A and 3B–3D). The residues involved in hydrogen bonding in the RelBDD homodimer are I286, N287, and Y300. The other residues located at or near the domain interface in RelBDD are C284, R285, H332, and I335.

Detailed investigation of the origin of the altered conformations of three aforementioned side chains in RelB provides the following insights. H332 in RelB cannot assume the same conformation as the equivalent His of other NF-κB proteins because Q334, which participates in the new crossdomain β strand formation, sterically blocks that position (compare Figures 2D and 2E).

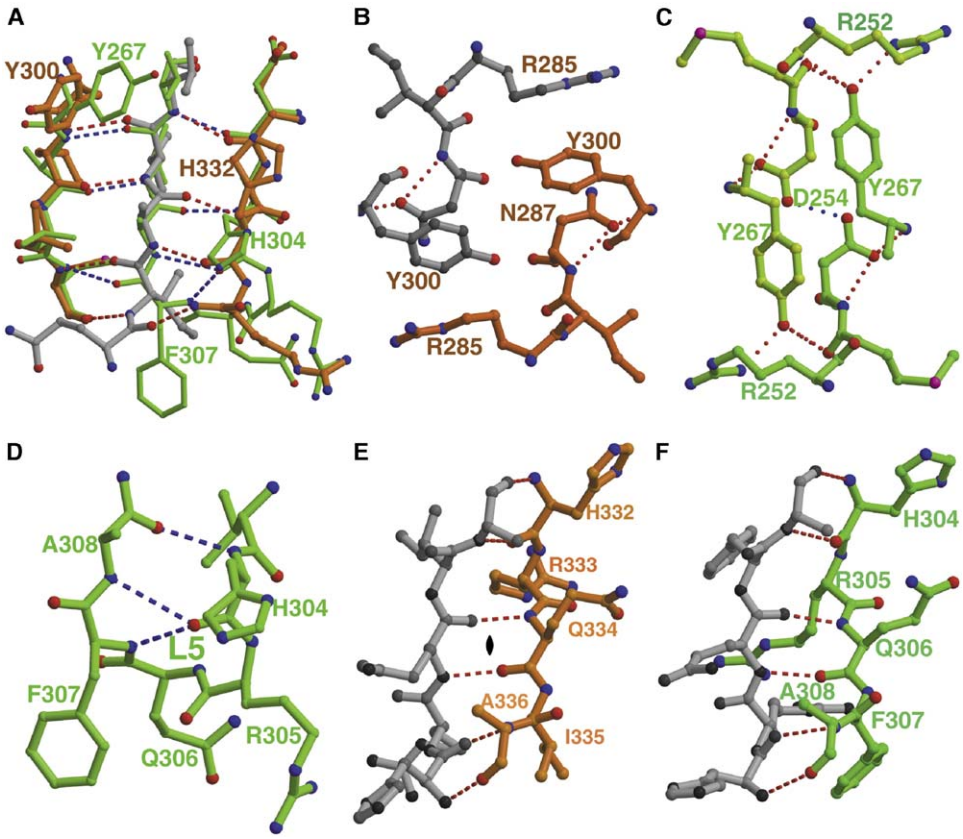

Figure 2. Detailed Structural Comparisons between the RelBDD Homodimer and the p50DD Homodimer

(A) Overlay of the "b"–"e" β sheets from p50DD and RelBDD . This view is generated by rotating the superimposed Ig-like folds (right) 90° around the long axis of the fold, as shown in Figure 1E. All of the p50 (green) residues are involved in the dimer interface. RelB is shown in red and gray, respectively, for the two chains in the β sheet.

(B and C) Comparison of the orientations of homologous Tyr at the subunit interfaces of the RelBDD and p50DD dimers, respectively.

(D) The β turn connecting β strands "c′" and "e" and the residues present in the turn of p50DD are shown.

(E) The same segment as in (C) in RelBDD is shown. The turn is converted into a strand ("d"), and the two opposing strands connecting the two Ig-like folds of RelBDD are presented. The side chain conformations of His and Gln are completely different in the two dimers.

(F) The hydrogen bonding pattern in the swapped region of the MLAM mutant of p50DD.

The Chi1 dihedral angles for residue Y267 in regular NF-κB dimers are around –80 (g+). In RelBDD, the angle is 65 (g–) for the corresponding Y300 residue. In p50DD, the distance between two Cα atoms of Y267 is 7 Å, whereas the distance between the same two atoms in RelBDD is 13 Å. If the Y300 in RelBDD adopts the g(+) conformation, it would not participate in dimer formation. On the other hand, if Y267 in p50DD adopts the g(–) conformation, the side chain atoms of the tyrosine will be too close to each other. One likely explanation for the conformational differences of this critical tyrosine residue might be that nonhomologous residue(s) at the RelB dimer interface may impose energetically unfavorable interactions if two RelB monomers associate in a manner similar to that of other NF-κB dimers. Therefore, given the restricted conformation imposed by the domain intertwining, the observed conformation is the most favorable one adopted by this residue in RelB.

Structure of RelBDD Y300S

We wanted to test if the conformation of RelBDD Y300 is the cause of the intertwined homodimer formation rather than the consequence of it. We mutated this residue into Ala and Ser and wanted to test the mutants by crystallographic analysis. Our effort to crystallize the alanine mutant was not successful. However, we successfully crystallized the serine mutant and determined the structure at 2.2 Å resolution. This mutant also forms an intertwined homodimer (Figure 3A). The open interface is more open than that in wild-type RelBDD. Superposition of wild-type RelBDD and RelBDD Y300S through one domain requires a 24° rotation and a 9 Å translation to fit the second domains onto each other (Figure 3B). The solvent-excluded surface area in the open interface is only 360 Å^2. The Cα atoms of two Ser in the mutants are farther apart compared to the same two atoms of Tyr in wild-type RelBDD (17 Å versus 13 Å) (Figure 3C). This observation suggests that Y300 does not induce intertwining. In fact, this residue contributes to the overall stability of the dimer.

RelB Is an Intertwined Dimer in Solution

To test if the RelBDD homodimer is indeed an intertwined homodimer in solution and if our observation is

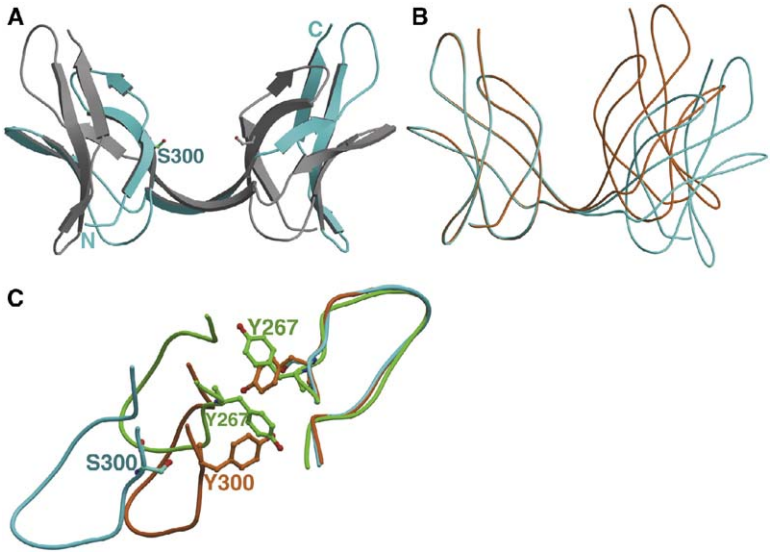

Figure 3. Structural Comparison between RelBDD and RelBDD Y300S

(A) Ribbon representation of the RelBDD Y300S homodimer. Gray and cyan, respectively, represent the two RelB subunits.

(B) Backbone overlay of RelBDD (orange) and RelBDD Y300S (cyan) by superimposing one subunit from each dimer. The open interface of the mutant is farther apart than the same interface in wild-type RelBDD.

(C) Comparison of the dimer interfaces of wild-type RelBDD, RelBDD Y300S, and p50DD centered around the tyrosine.

not simply an artifact of crystallization, we have designed strategically placed cysteine mutations and tested covalent crosslinking of the mutant. The side chains of two surface residues, D310 and T363, are only 4 Å apart in RelBDD, and we have mutated these residues to Cys (RelBDD-Cys), as shown in Figure 4 (left). An intermolecular disulfide bond will be formed, connecting the two polypeptide chains, only if RelBDD-Cys forms an intertwined dimer. In contrast, if each chain is folded independently, then an intramolecular disulfide bond will form. The mutant was denatured and then refolded in the presence of DTT. DTT was then removed by gel filtration, allowing the spontaneous formation of disulfide bonds in an oxidizing environment. The samples were analyzed in a nonreducing SDS-PAGE gel. We observed that under this condition, a significant amount of RelBDD-Cys is present as a dimer (Figure 4, right, lane 3). Wild-type RelBDD migrates as a monomer in the gel. As a control, we have generated the cysteine mutations at the corresponding positions in p52DD, and the p52DD-Cys mutant was subjected to identical treatment as RelBDD-Cys. As expected, we do not observe any p52 dimer (Figure 4, right, lane 5). These results demonstrate that RelBDD forms an intertwined dimer in solution, whereas the p52DD dimer is formed by the association of two independently folded monomers.

Why Does RelB Form an Intertwined Dimer?

Although a clear mechanism for RelB intertwined dimer formation requires additional mutational and biophysical experiments, the structures presented here, along with the structure of the p50DD MLAM mutant, provide some insights. The domain swapping in the p50DD mutant appears to be caused by the replacement of a large side chain (valine to methionine) at position 310 that induces a steric clash in the process of regular dimer formation. Domain swapping in the p50DD dimer relieves the clash (Chirgadze et al., 2004). In RelB, all dimer-forming residues present in p50, including Y267, L269, A308, and V310, are conserved. Therefore, the inability to undergo side-by-side RelB homodimer for-

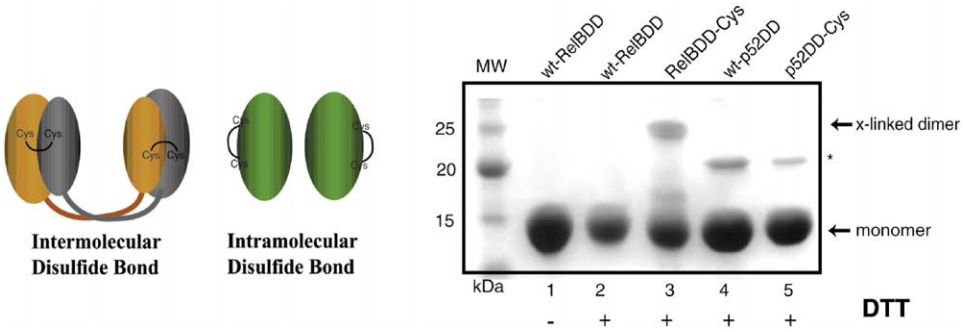

Figure 4. RelDD is an Intertwined Homodimer in Solution

Left: a schematic of intramolecular versus intermolecular crosslinking. Right: Coomassie-stained, nonreducing SDS-polyacrylamide gel after separating the crosslinked dimer from the monomer. Lane 1, MW standard; lane 2, wild-type RelBDD in the absence of DTT; lane 3, wild-type RelBDD in the presence of DTT; lane 4, RelBDD-Cys in the presence of DTT; lane 5, wild-type p52DD in the presence of DTT; lane 6, p52DD-Cys in the presence of DTT. The asterisks denote unknown protein bands. RelBDD proteins are fused to a polyhistidine tag.

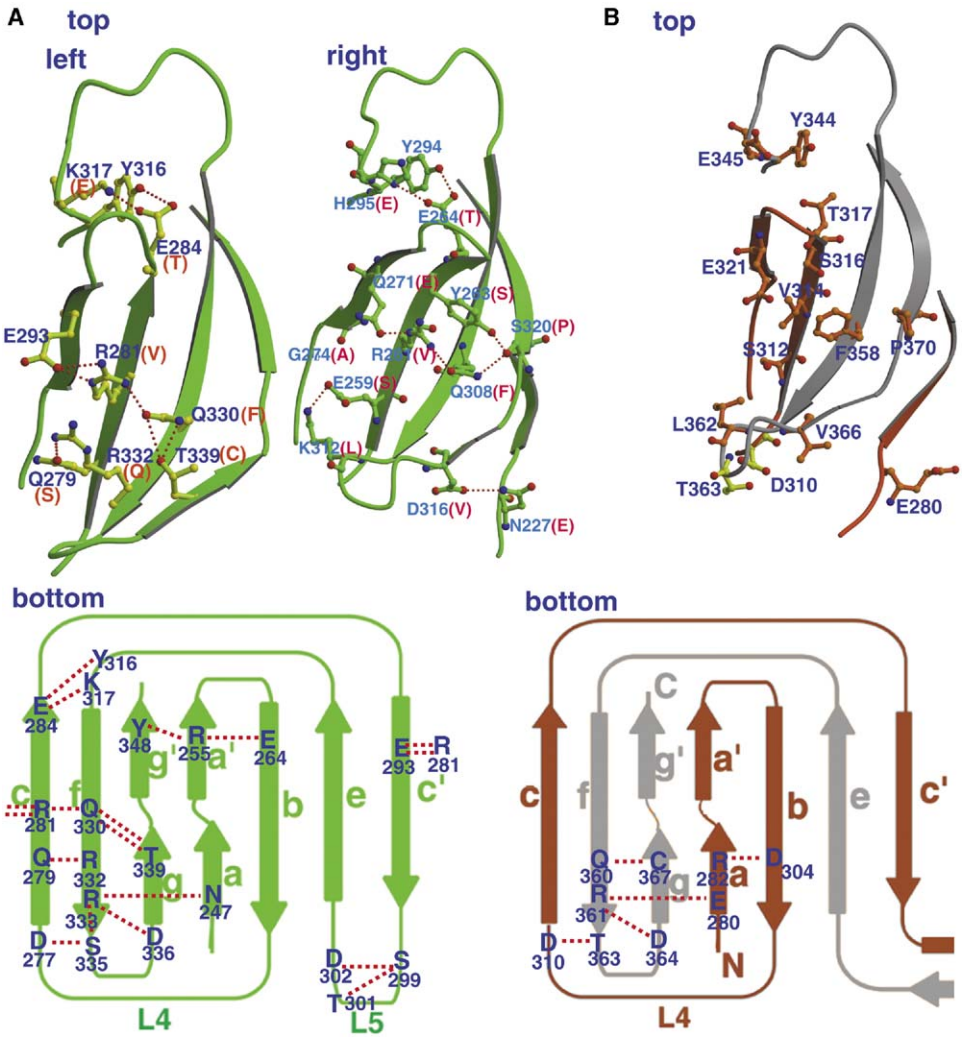

Figure 5. Surface Hydrogen Bonding Patterns Are Different between p50DD and RelBDD

(A) (Top, left) A section of the p50DD surface is shown. All of the side chain-to-side chain surface hydrogen bonds (dotted lines) seen within this section of the p50DD surface are shown. (Top, right) The same section of the p52DD surface as in p50DD (left) as well as the hydrogen bonds are shown. Corresponding residues in RelB are shown in parentheses. (Bottom) A schematic showing all 14 side chain-to-side chain surface hydrogen bonds in p50DD.

(B) (Top) The identical section of the RelBDD surface as p50DD and p52DD (A) is shown. No side chain-to-side chain surface hydrogen bond is present in this section of RelBDD. D310 and T363 (in yellow) are residues used for disulfide trapping. (Bottom) All five side chain-to-side chain hydrogen bonds in a RelBDD Ig-like fold are shown as a schematic drawing.

mation might not be due to any steric clash. We propose that the low stability of the RelBDD monomer is at least partly responsible for domain swapping in the RelBDD dimer. Although pairwise sequence comparisons do not reveal any striking differences between RelB and other NF-κB family subunits, some surface amino acids are altered in RelB (Figure 1A). The surface polar residues in nonRelB NF-κB subunits form a hydrogen bonding network that links distal secondary structures, resulting in a stable domain structure (Figure 5A). In RelBDD, only five intradomain side chain-to-side chain surface hydrogen bonds are observed (Figure 5B). In contrast, 14 such bonds are observed in p50 and p52. It has been shown in several systems that surface hydrogen bonds contribute to the overall domain folding stability (Pokkuluri et al., 2002; Takano et al., 1999). It is likely that stable folding of RelBDD requires additional energy that is gained by creating an extra β sheet in the intertwined homodimer. The structure of RelBDD Y300S demonstrates that interactions at the open dimer interface are also important for the overall stability of the dimer. Our preliminary unfolding studies show that the folding stability of the RelBDD dimer is similar to that of the p52DD dimer (data not shown). These observations are consistent with results from other studies that show that increased entropy of the monomer and the addition of new interactions at hinge loops can favor the formation of an intertwined dimer (Liu and Eisenberg, 2002; Rousseau et al., 2003). The high sequence conservation within strand "d"

among the Rel proteins suggests that this sequence at the hinge/strand region may further facilitate intertwining in Rel proteins.

RelB Homo- and Heterodimers

If the RelBDD dimer is a relatively strong RelB dimer, why does RelB then fail to form a functional stable homodimer in vivo? We suggest that the relative lack of stability of the N-terminal domain of the RHR and the leucine zipper (LZ) domain may contribute to the overall instability of the RelB homodimer in vivo. Earlier reports have shown that RelB is degraded through the sequential action of calpain and proteasome (Marienfeld et al., 2001). The initial cleavage site is located within the N-terminal leucine zipper domain. It is possible that RelB is degraded easily by the proteasome after initial cleavage by calpain. Interestingly, we have observed that, in contrast to RelBDD and other NF-κB RHRs, the RelB RHR is difficult to purify as a stable protein from *E. coli*. This protein continuously degrades during the course of expression and purification. One possible explanation is that the N-terminal domain of RelB makes this protein degradation sensitive both in *E. coli* and in mammalian cells. RelB stabilizes itself by associating with p50 and p52 in vivo. Consistent with in vivo stability, we also observe that RelB/p50 and RelB/p52 heterodimers are stable proteins and are easy to purify from an *E. coli* expression system (data not shown). One possibility is that the proteolytically sensitive region of RelB is protected by p50 and p52.

Regulation of NF-κB Dimer Formation

Combinatorial association between the members of a protein family broadens the scope of these oligomeric proteins' activity and hence diversifies their biological functions. Perhaps the clearest example of such diversification comes from families of transcription factors. It is well known that different dimeric transcription factors belonging to a family regulate gene expression with distinct properties. These distinct biological properties are achieved by alteration in DNA binding affinity and specificity, by interactions with other activators bound to neighboring DNA sites, and by recruitment of coactivators. NF-κB is one such transcription factor family in which the homo- and heterodimers display distinct biological functions.

It has been known for a long time that different NF-κB dimers have different strengths. Our previous experiments revealed differential strengths of various NF-κB dimers in the canonical pathway, and crystallographic analyses provided a molecular basis for such differences. For example, the p50/p65 heterodimer is roughly 7- and 4-fold stronger than the p65 and p50 homodimers, respectively (Phelps et al., 2000). However, the oncogenic NF-κB v-Rel protein reveals an unusual dimerization property. Although v-Rel and its protooncogenic form c-Rel (chicken) differ by only three amino acids within the dimerization domain, their dimerization properties are different (Phelps and Ghosh, 2004). Whereas the v-Rel homodimer and the v-Rel/p50 heterodimer are of nearly equal strengths, c-Rel forms a preferential heterodimer with p50. Surprisingly, these altered amino acids are located outside of the typical NF-κB subunit interface.

If one considers an NF-κB specificity spectrum, p65 and RelB, the critical components of canonical and noncanonical pathways, respectively, lie at the two extreme ends. RelB exhibits *high* specificity for p100/p52 and p105/p50 and is nonexistent in their absence. On the other hand, p65 exhibits *low* specificity, and, in the absence of its preferential dimeric partner, p50, it still can form a functional homodimer (Hoffmann et al., 2003). This marked difference in specificity might then define the effective range of the canonical and noncanonical pathways. The canonical pathway is broad, regulating a large number of genes, and is involved in many biological functions. The noncanonical pathway is narrow, regulating only a limited set of genes, and is essential for a highly specific function.

The X-ray structure presented here reveals that the RelB dimerization domain forms a stable homodimer through intertwining. We suggest that the relative lack of stability of the RelBDD fold appears to induce the formation of a three-dimensional domain-swapped homodimer rather than a classical side-by-side dimer. An unstable RelB monomer might be essential for the formation of two physiological NF-κB heterodimers, RelB/p50 or RelB/p52. These two RelB-specific heterodimers have distinct physiological roles. RelB/p50 is constitutively nuclear and functions primarily as a repressor, whereas the RelB/p52 heterodimer is formed in response to specific inducers and functions as an activator of transcription (Bours, 1999; Marienfeld et al., 2003; Suhasini and Pilz, 1999). Based on the architecture of the RelB homodimer, it is apparent that the RelB homodimer must be unfolded before it associates with p50 and p52. Therefore, it is likely that the RelB/p50 and RelB/p52 heteordimers are formed in vivo during domain folding. In the absence of p52 and p50, RelB forms a highly intertwined homodimer that is degraded by cellular proteases as well as by the proteasome. At this time, it is difficult to say if the RelB homodimer has any functional role in vivo. We suggest that the transiently stable RelB homodimer might prevent its rapid degradation, allowing sufficient time for heterodimer formation with p50 and p52. Additional experiments are needed to validate this suggestion.

Experimental Procedures

Protein Expression and Crystallization

We subcloned the dimerization domain of RelB (RelBDD, residues 278–393) into the T7 polymerase-based vector pET15b to express RelBDD as a fusion protein tagged with an additional 21 residues, including a hexa-histidine tag. *E. coli* cells harboring the expression plasmid were grown to an OD_{600} of ~0.5 at 37°C, followed by induction with 100 μM IPTG. Cells were grown continuously postinduction at room temperature for 12–16 hr. The His-tagged RelBDD was purified in two chromatographic steps: an affinity step with Ni-agarose resin (Novagen), followed by size exclusion (Superdex 75, Amersham-Pharmacia). Crystals were grown by the hanging drop vapor diffusion method with 4 μl of a 1:1 mixture of protein solution and a well solution at 18°C. The drop was equilibrated against a well solution composed of 22% PEG 8000, 0.1 M ammonium sulfate, and 0.1M cacodylate buffer (pH 6.5). The initial protein concentration in the crystallization drops was 8 mg/ml. 0.2 × 0.2 × 0.1 mm crystals were grown within 3–4 days. RelBDD Y300A was purified by using same procedure as that for wild-type RelBDD. Crys-

Table 1. Summary of Crystallographic Analysis

	RelBDD	Y300S
Data Collection		
Space group	$P3_121$	$P3_121$
Unit cell (Å)		
a	69.20	75.61
b	69.20	75.61
c	64.74	65.33
Volume (Å^3)	268,482	323,446
Resolution (Å)	2.18 (2.26–2.18)	2.20 (2.28–2.20)
I/σ	7.8 (2.5)	12.3 (2)
Completeness (%)	100 (99)	94 (60)
R_{symm}[a] (%)	6.1 (45.9)	5.0 (47.4)
Refinement		
Number of reflections	8,226	8,784
Number of protein atoms	869	863
Number of waters	103	62
$R_{crystal}$[b] (%)	19.5	20.6
R_{free}[c] (%)	21.8	23.1
Rmsd		
Bond length (Å)	0.006	0.006
Bond angle (°)	1.47	1.42
Ramachandran plot (%)		
Most favored regions	93	92
Additionally allowed regions	7	8
Disallowed regions	0	0

[a] $R_{symm} = \Sigma|I_{obs} - I_{avg}|/\Sigma I_{avg}$.
[b] $R_{cryst} = \Sigma||F_{obs}| - |F_{calc}||/\Sigma F_{obs}$.
[c] R_{free} was calculated with 10% of data.

tals of the mutant were grown by using a 1:1 mixture of 10 mg/ml protein with a well solution composed of 22% PEG 8000, 0.1 M ammonium sulfate, and 0.1 M cacodylate buffer (pH 6.5).

Data Collection and Structure Solution

For RelBDD, X-ray diffraction data were collected by using a MAR345 imaging plate mounted on a Rigaku rotating anode. Before being flash frozen under a liquid nitrogen stream for data collection at 105 K, the crystals were soaked in solutions containing all of the components of the mother liquor plus glycerol, the concentration of which was increased from 5% to 28% in about 10 min. The diffraction pattern showed that the crystal belonged to the trigonal system, with the unit cell a = 69.20 Å, c = 64.74 Å, and possible space groups of $P3_121$ or $P3_221$. There is only one monomer in an asymmetric unit, and it has a solvent volume fraction of 0.66. The data were indexed and integrated with DENZO and were scaled with SCALEPACK (Otwinowski, 1993; Otwinowski and Minor, 1997). Table 1 lists the data processing statistics.

The structure was determined by molecular replacement with AMORE, and a monomer of p65DD was used as the search model (Navaza, 2001). The solution was obtained in space group $P3_121$. The molecular replacement solution was top peak, with 5.8 σ in the rotation function and 10.4 σ in the translation function. Rigid body fitting of the solution in AMORE gave an R factor of 45.5% in the 10.0–4.0 Å resolution range. The orientation and position of the initial model were further refined by rigid-body refinement in CNS (Brunger et al., 1998). The amino acid sequence was replaced with RelB based on $2F_o$-F_c maps by using the programs O and X-talView (Jones et al., 1991; McRee, 1999). The structure was refined by using minimization and simulated annealing with a maximum likelihood target function and a flat bulk solvent correction with CNS. During model rebuilding, the 2Fo-Fc and Fo-Fc maps revealed that R333 in one monomer might connect to Q334 in the other monomer with a perfect electron density fitting. The connecting of main chain atoms from one monomer to those of the other monomer leads to an intertwined dimer. The following refinements showed that the intertwined model is much better than the regular dimer in terms of all crystallographic evidences of electron density fitting, temperature factors, R factors, and geometries. When individual temperature factors were included in the refinement, the final R factor was 19.5% and the R_{free} was 21.8% for 20.0–2.18 Å data. The ϕ/ψ angles of all of the residues are in the most favored regions (93%) and additionally allowed regions (7%) in the Ramachandran plot.

The RelBDD Y300S mutant was created by using a kit and by following the method described by the manufacturer (Amersham-Pharmacia). The mutant was expressed in *E. coli* and was purified by using the procedure described for the wild-type protein. The structure of the RelBDD Y300S mutant was also determined by molecular replacement by using the domain of the RelBDD dimer as a search model. The detailed results of the refinement are shown in Table 1.

Crosslinking

Proteins were unfolded at 0.3 mg/ml concentration in denaturing buffer (8 M urea, 50 mM Tris-HCl [pH 8.0], 500 mM NaCl, 5 mM DTT), followed by slow refolding by dialyzing three times against the same buffer without urea. Salt was reduced to 50 mM in the final dialysis step. Proteins were then concentrated to 1 mg/ml, followed by incubation of the samples in 20 mM DTT, 50 mM Tris-HCl (pH 8.0) on ice for 1 hr. DTT was removed by passing the reaction mixture through a Sephadex G-25 centrifuge column equilibrated with the same buffer. Nonreducing gel loading buffer was added prior to running the samples on an 18% SDS-polyacrylamide gel. Protein was visualized by Coomassie staining.

Acknowledgments

We thank Anu K. Moorthy, Tom Huxford, and Partho Ghosh for critically reading the manuscript. We also thank the Keck computer facility and Robert Konecny for his support in the structural and graphical work. G.G. thanks Joan Wu and Arthur Hacket, two past undergraduate researchers in the lab, for their efforts on expression cloning, protein purification, and crystallization. This work is supported by funding from the National Institutes of Health (National Cancer Institute and Allergy and Immunology) and the university-wide AIDS research program.

Received: March 24, 2005
Revised: June 14, 2005
Accepted: June 15, 2005
Published: September 13, 2005

References

Baldwin, A.S., Jr. (1996). The NF-κ B and I κ B proteins: new discoveries and insights. Annu. Rev. Immunol. *14*, 649–683.

Bennett, M.J., and Eisenberg, D. (1994). Refined structure of monomeric diphtheria toxin at 2.3 Å resolution. Protein Sci. *3*, 1464–1475.

Bours, V. (1999). NF-κ B and cancers. Bull. Mem. Acad. R. Med. Belg. *154*, 335–345.

Brunger, A.T., Adams, P.D., Clore, G.M., DeLano, W.L., Gros, P., Grosse-Kunstleve, R.W., Jiang, J.S., Kuszewski, J., Nilges, M., Pannu, N.S., et al. (1998). Crystallography & NMR system: a new software suite for macromolecular structure determination. Acta Crystallogr. D Biol. Crystallogr. *54*, 905–921.

Chen, F.E., and Ghosh, G. (1999). Regulation of DNA binding by Rel/NF-κB transcription factors: structural views. Oncogene *18*, 6845–6852.

Chen, F.E., Huang, D.B., Chen, Y.Q., and Ghosh, G. (1998a). Crystal structure of p50/p65 heterodimer of transcription factor NF-κB bound to DNA. Nature *391*, 410–413.

Chen, Y.Q., Ghosh, S., and Ghosh, G. (1998b). A novel DNA recognition mode by the NF-κ B p65 homodimer. Nat. Struct. Biol. *5*, 67–73.

Chirgadze, D.Y., Demydchuk, M., Becker, M., Moran, S., and Paoli, M. (2004). Snapshot of protein structure evolution reveals conservation of functional dimerization through intertwined folding. Structure (Camb) *12*, 1489–1494.

Claudio, E., Brown, K., Park, S., Wang, H., and Siebenlist, U. (2002). BAFF-induced NEMO-independent processing of NF-κ B2 in maturing B cells. Nat. Immunol. *3*, 958–965.

Coope, H.J., Atkinson, P.G., Huhse, B., Belich, M., Janzen, J., Holman, M.J., Klaus, G.G., Johnston, L.H., and Ley, S.C. (2002). CD40 regulates the processing of NF-κB2 p100 to p52. EMBO J. *21*, 5375–5385.

Cramer, P., Larson, C.J., Verdine, G.L., and Muller, C.W. (1997). Structure of the human NF-κB p52 homodimer-DNA complex at 2.1 Å resolution. EMBO J. *16*, 7078–7090.

Dejardin, E., Droin, N.M., Delhase, M., Haas, E., Cao, Y., Makris, C., Li, Z.W., Karin, M., Ware, C.F., and Green, D.R. (2002). The lymphotoxin-beta receptor induces different patterns of gene expression via two NF-κB pathways. Immunity *17*, 525–535.

de Lumley, M., Hart, D.J., Cooper, M.A., Symeonides, S., and Blackburn, J.M. (2004). A biophysical characterisation of factors controlling dimerisation and selectivity in the NF-κB and NFAT families. J. Mol. Biol. *339*, 1059–1075.

Ghosh, S., and Karin, M. (2002). Missing pieces in the NF-κB puzzle. Cell *109* (*Suppl.*), S81–S96.

Ghosh, G., van Duyne, G., Ghosh, S., and Sigler, P.B. (1995). Structure of NF-κ B p50 homodimer bound to a κ B site. Nature *373*, 303–310.

Ghosh, S., May, M.J., and Kopp, E.B. (1998). NF-κ B and Rel proteins: evolutionarily conserved mediators of immune responses. Annu. Rev. Immunol. *16*, 225–260.

Gerondakis, S., Grossmann, M., Nakamura, Y., Pohl, T., and Grumont, R. (1999). Genetic approaches in mice to understand Rel/NF-κB and IκB function: transgenics and knockouts. Oncogene *18*, 6888–6895.

Hart, D.J., Speight, R.E., Sutherland, J.D., and Blackburn, J.M. (2001). Analysis of the NF-κB p50 dimer interface by diversity screening. J. Mol. Biol. *310*, 563–575.

Hoffmann, A., Leung, T.H., and Baltimore, D. (2003). Genetic analysis of NF-κB/Rel transcription factors defines functional specificities. EMBO J. *22*, 5530–5539.

Huang, D.B., Huxford, T., Chen, Y.Q., and Ghosh, G. (1997). The role of DNA in the mechanism of NFκB dimer formation: crystal structures of the dimerization domains of the p50 and p65 subunits. Structure *5*, 1427–1436.

Huang, D.B., Chen, Y.Q., Ruetsche, M., Phelps, C.B., and Ghosh, G. (2001). X-ray crystal structure of proto-oncogene product c-Rel bound to the CD28 response element of IL-2. Structure (Camb.) *9*, 669–678.

Liu, Y., and Eisenberg, D. (2002). 3D domain swapping: as domains continue to swap. Protein Sci. *11*, 1285–1299.

Jones, T.A., Zou, J.Y., and Cowan, S.W. (1991). Improved methods for building protein models in electron density maps and the location of errors in these models. Acta Crystallogr. A *47*, 110–119.

Karin, M., and Ben-Neriah, Y. (2000). Phosphorylation meets ubiquitination: the control of NF-[κ]B activity. Annu. Rev. Immunol. *18*, 621–663.

Marienfeld, R., Berberich-Siebelt, F., Berberich, I., Denk, A., Serfling, E., and Neumann, M. (2001). Signal-specific and phosphorylation-dependent RelB degradation: a potential mechanism of NF-κB control. Oncogene *20*, 8142–8147.

Marienfeld, R., May, M.J., Berberich, I., Serfling, E., Ghosh, S., and Neumann, M. (2003). RelB forms transcriptionally inactive complexes with RelA/p65. J. Biol. Chem. *278*, 19852–19860.

McRee, D.E. (1999). XtalView/Xfit–a versatile program for manipulating atomic coordinates and electron density. J. Struct. Biol. *125*, 156–165.

Muller, C.W., Rey, F.A., Sodeoka, M., Verdine, G.L., and Harrison, S.C. (1995). Structure of the NF-κ B p50 homodimer bound to DNA. Nature *373*, 311–317.

Navaza, J. (2001). Implementation of molecular replacement in AMoRe. Acta Crystallogr. D Biol. Crystallogr. *57*, 1367–1372.

Otwinowski, Z. (1993). DENZO: An Oscillation Data Processing Program for Macromolecular Crystallography (New Haven, CT: Yale University Press).

Otwinowski, Z., and Minor, W. (1997). Processing of X-ray diffraction data collected in oscillation mode. In Methods in Enzymology, R.M. Sweet and C.W. Carter, eds. (New York: Academic Press), pp. 307–326.

Phelps, C.B., and Ghosh, G. (2004). Discreet mutations from c-Rel to v-Rel alter κB DNA recognition, IκBα binding, and dimerization: implications for v-Rel oncogenicity. Oncogene *23*, 1229–1238.

Phelps, C.B., Sengchanthalangsy, L.L., Malek, S., and Ghosh, G. (2000). Mechanism of κ B DNA binding by Rel/NF-κ B dimers. J. Biol. Chem. *275*, 24392–24399.

Pokkuluri, P.R., Raffen, R., Dieckman, L., Boogaard, C., Stevens, F.J., and Schiffer, M. (2002). Increasing protein stability by polar surface residues: domain-wide consequences of interactions within a loop. Biophys. J. *82*, 391–398.

Rousseau, F., Schymkowitz, J.W., and Itzhaki, L.S. (2003). The unfolding story of three-dimensional domain swapping. Structure (Camb) *11*, 243–251.

Ruben, S.M., Klement, J.F., Coleman, T.A., Maher, M., Chen, C.H., and Rosen, C.A. (1992). I-Rel: a novel rel-related protein that inhibits NF-κ B transcriptional activity. Genes Dev. *6*, 745–760.

Ryseck, R.P., Novotny, J., and Bravo, R. (1995). Characterization of elements determining the dimerization properties of RelB and p50. Mol. Cell. Biol. *15*, 3100–3109.

Sanjabi, S., Hoffmann, A., Liou, H.C., Baltimore, D., and Smale, S.T. (2000). Selective requirement for c-Rel during IL-12 P40 gene induction in macrophages. Proc. Natl. Acad. Sci. USA *97*, 12705–12710.

Senftleben, U., Cao, Y., Xiao, G., Greten, F.R., Krahn, G., Bonizzi, G., Chen, Y., Hu, Y., Fong, A., Sun, S.C., and Karin, M. (2001). Activation by IKKα of a second, evolutionary conserved, NF-κ B signaling pathway. Science *293*, 1495–1499.

Sengchanthalangsy, L.L., Datta, S., Huang, D.B., Anderson, E., Braswell, E.H., and Ghosh, G. (1999). Characterization of the dimer interface of transcription factor NFκB p50 homodimer. J. Mol. Biol. *289*, 1029–1040.

Suhasini, M., and Pilz, R.B. (1999). Transcriptional elongation of c-myb is regulated by NF-κB (p50/RelB). Oncogene *18*, 7360–7369.

Takano, K., Yamagata, Y., Kubota, M., Funahashi, J., Fujii, S., and Yutani, K. (1999). Contribution of hydrogen bonds to the conformational stability of human lysozyme: calorimetry and X-ray analysis of six Ser → Ala mutants. Biochemistry *38*, 6623–6629.

Xiao, G., Harhaj, E.W., and Sun, S.C. (2001). NF-κB-inducing kinase regulates the processing of NF-κB2 p100. Mol. Cell *7*, 401–409.

Accession Numbers

The coordinates of the two structures have been deposited into the Protein Data Bank under codes RelBDD (1ZK9) and RelB Y300S (1ZKA).